RC22365 (W0203-033) March 11, 2002
Materials Science

IBM Research Report

The Phase Transformation of Thin Sputter-deposited Tungsten Films at Room Temperature

Stephen M. Rossnagel, I. Cevdet Noyan, Cyril Cabral, Jr.
IBM Research Division
Thomas J. Watson Research Center
P.O. Box 218
Yorktown Heights, NY 10598

Research Division
Almaden - Austin - Beijing - Haifa - India - T. J. Watson - Tokyo - Zurich

LIMITED DISTRIBUTION NOTICE: This report has been submitted for publication outside of IBM and will probably be copyrighted if accepted for publication. Ithas been issued as a Research Report for early dissemination of its contents. In view of the transfer of copyright to the outside publisher, its distributionoutside of IBM prior to publication should be limited to peer communications and specific requests. After outside publication, requests should be filled only by reprints or legally obtained copies of the article (e.g. payment of royalties). Copies may be requested from IBM T. J. Watson Research Center , P. O. Box 218, Yorktown Heights, NY 10598 USA (email: reports@us.ibm.com). Some reports are available on the internet at http://domino.watson.ibm.com/library/CyberDig.nsf/home

The Phase Transformation of Thin Sputter-deposited Tungsten Films at Room Temperature

S.M. Rossnagel, I.C. Noyan and C. Cabral. Jr.
IBM Research Division
PO 218
Yorktown Heights NY 10598

ABSTRACT

Thin films of W have been deposited by sputtering (PVD) at near-room temperature, using Ar as the working gas, for evaluation of the electrical and structural properties of the films in the thickness range of 3 to 150 nm. Films deposited at 45 nm or greater thickness are composed of alpha (bcc) phase (only) with an electrical resistivity of 12 micro-Ohm-cm. Films deposited at thicknesses below 5 nm are mostly beta (A15 cubic) phase as-deposited with significantly higher resistivity, which is due partly to the phase and partly to electron-surface scattering (the 'size effect'). In the thickness range of 5 to 45 nm, the as-deposited films are mostly beta-phase and undergo transformation to the alpha phase at room temperature in tens of hours to several days. The resistivity also declines concurrently, as much as 70%. The exact mechanism driving the phase transformation is unclear, but is expected to be due to energy stored at grain boundaries and at the film-substrate interface coupled with the metastable nature of the beta phase. The transition is thermally driven and can be enhanced by heating or slowed by cooling. The effective activation energy for the phase transformation measured by the modified Kissenger method for the change in sheet resistance, the disappearance of the W-beta peaks, or the appearance of the W-alpha peaks has an average value of 1.1 +/- 0.2 eV. It does not appear that there is any critical thickness for the transition. However, since the deposition process for PVD-W is intrinsically hot, thicker films are effectively deposited at higher temperatures, which drives the beta-to-alpha transition to completion. Thicker films deposited cold (<20C) show beta-phase peaks, which then transform to alpha in 10-20 hours at 25C. In addition, the scaling of the resistivity of the resultant alpha W with thickness suggests an electron scattering mean-free-path of 10-12 nm, much below the reported 41 nm (1)

INTRODUCTION

Thin, conformal films of various refractory materials (Ti, TiN, Ta, TaN, W, WN, etc) are routinely used in semiconductor fabrication as diffusion barriers or 'liners', adhesion layers, and potentially seed layers. While the materials are generally too resistive to be used as the primary conductor in all but the contact level, their conductivity must be high enough to allow significant current flow through the film. This is most critical at the bottom of a via, where the diffusion barrier is in series with the Cu or Al(Cu) via electrically. In the Cu interconnect system, generally diffusion barriers of Ta and TaN are used (2), although the W and WN systems are also interesting. The Al(Cu) system generally uses Ti and TiN barriers.

In semiconductor integrated circuit manufacturing, the bulk of the deposition of these refractory materials has been by sputter deposition, also known generically as Physical Vapor Deposition

(PVD), although that term is also used outside of the semiconductor industry for evaporative deposition as well. To enhance the conformality of the deposited films, PVD has been modified either by the introduction of filters or collimators (3), by long throw distances (4-5) or by the use of ionization of the sputtered metal atoms (6-9). While increasing the directionality of the deposition by these techniques seems initially counterintuitive to the deposition of a more conformal film, the more-normal deposition facilitates a more conformal deposition by eliminating large overhangs at the tops of trenches and vias which block deposition from the lower areas of the structure. There is also a modest increase in Ta atom reflectivity at high deposition angles, which can lead to better conformality in deep, steep-walled vias when the Ta arrives close to normal incidence (5).

The sputter deposition of metal onto a damascene-type interconnect structure, such as a trench or via, results in a much thicker deposit in the planar or field area between the inset vias or trenches than on the sidewalls and bottoms the those features. The ratio of the deposition in the features, compared to the planar areas, is known as the step coverage. For moderate aspect ratio (AR = feature depth/feature width) features of AR= 3 or so, the step coverage on the sidewalls is at most 10-15%. For a field thickness deposit of 30-40 nm, this results in a functional film thickness on the sidewalls of 3-6 nm per layer. The eventual barrier/liner stack sidewall thickness in real interconnect structures is then on the order of 10 nm or less.

Films in the 10 nm range are likely to have significantly higher resistivity than either thick films or bulk samples of the same material. This is due to the scattering of conduction electrons from the film surfaces (10), and is often described generically as the 'size effect.'. A relation for the film resistivity, ρ, of thickness t, that describes this effect is given as (11):

$$\rho = \rho_b (1 + 0.375 \lambda(1\text{-}p)/t) \qquad (1)$$

Where ρ_b is the resistivity of the bulk material, λ is the electron mean free path, and p is the scattering coefficient at the surface, which varies from 0 for diffuse scattering to 1 for purely elastic scattering. Unfortunately, for most thin film materials, it appears that p is purely diffuse and as such, the size-dependent scattering effects are maximized (11).

Additional modifications to the resistivity of pure materials can be due to grain boundary scattering as well as surface roughness. A general form of the net resistivity for a 1:1 aspect ratio line of width d, from Kuan et al is: (11)

$$\rho_l = \rho_b (1 + 0.75 \lambda(1\text{-}p) S /d + 1.5 [R/(1\text{-}R)] \lambda /g) \qquad (2)$$

Where S is the surface scattering coefficient, R is the grain boundary scattering coefficient, and g is the average grain size of the material. The surface scattering coefficient is 1 for a smooth surface, and increases slowly due to roughness (11). The grain boundary scattering coefficient describes how much a grain boundary functions as a discrete surface, and ranges from 0 for no scattering to 1.0 for complete, surface-like scattering. For many materials, such as Cu, the value

for R is 0.3-0.5, and some results suggest that the value may be dependent on film dimensions (1).

TUNGSTEN

Films of tungsten have been deposited and characterized extensively in the literature. The properties of the film depend strongly on the deposition process as well as the film purity. The films are typically deposited as single-phase alpha-W which has the equilibrium bcc structure, as single-phase beta-W which has a A15 (cubic) structure, or mixtures of these two phases. (12) The resultant phase has been reported to depend strongly on film thickness, oxygen partial pressure in the chamber, substrate bias, temperature, and deposition power (13-14). In some cases, there is reported an empirical critical thickness, generally around 50 nm, after which the film transforms from the beta to the alpha phase and further deposition occurs only in this phase (12,15). The transformation has been widely characterized as a thermal process, and can be enhanced by annealing the samples in an oxygen-free environment at 150-200C (13). Occasional reports of phase transitions near room temperature have been reported over very long time periods (14,15).

The alpha-W phase has a bulk resistivity of 5.3 micro-Ohm-cm, although thin film deposition of the material has rarely resulted in near-bulk properties. One case of a thin film deposition approaching bulk resistivity values was for an elevated temperature epitaxial-like deposition (16). Typically, sputtered or CVD-W films (using WF_6 and hydrogen) have resistivities of 11-12 micro-Ohm-Cm at best and more commonly 20 micro-Ohm-cm or more. W films are particularly sensitive to impurities and reports of the incremental increase in resistivity due to impurity incorporation are in the range of 1.1 to 4.2 nano-Ohm-cm/ppm wt (where ppm wt is the impurity level by weight). (17-19).

The formation of beta-W has been reported to be very strongly influenced or stabilized by oxygen contamination in the film. Beta-W films are also reported to have significantly higher resistivity, as much as 150-350 micro-Ohm-cm (13).

EXPERIMENT

Thin films of W were deposited by magnetron sputter deposition in a commercial Applied Materials Endura chamber, using a planar, rotating-magnet W cathode (99.95% purity) with a diameter of 33 cm located a distance of 10 cm from the sample. The deposition power was 2.5 kW at an Ar pressure of 1 mTorr. The samples were oxidized Si wafers (200 mm) and fragments of wafers which were clamped to a heated/cooled 200 mm diameter platform. Samples were introduced through a loadlock, and the chamber base pressure was typically 1×10^{-7} Torr. The deposition rate under these conditions was 73 nm/min. The rate was calculated by measuring thicker films by a step profilometer and confirmed by Rutherford Backscattering. Following deposition electrical resistivity was measured with a 4 Pt. Probe, and x-ray diffraction was measured using a Philips XRD tool. Time resolved x-ray diffraction and resistive analysis was conducted at the National Synchrotron Light Source, Brookhaven National Laboratory,

monitoring the W-beta and W-alpha diffraction peaks along with resistance as a function of temperature at different heater ramp rates. The effective activation energies were calculted with the modified Kissenger method.

The resistivity of the as-deposited films is shown in Fig. 1 as a function of film thickness up to 150 nm. Films thicker than 150 nm generally delaminated from the silicon dioxide substrate surface due to excessive compressive stress. As nominally expected, the resistivity climbs rapidly as the film thickness is reduced. However, no real changes were observed until the thickness was reduced below 50 nm. This is somewhat inconsistent with reported electron mean-free-paths in W of 41 nm (1, 17). From the general model of Eqn (1), a film thickness on the order of the mean free path would show an increase of at least 40% due to just thickness alone. Surface roughness and grain boundary scattering events would increase this amount. However, while the resistivity is roughly 2x the bulk value, it is most likely that the high baseline in Fig. 1 is due to systematic impurities, since it does not show a thickness dependence at >40 nm. This suggests that the thick film resistivity is not directly due to surface roughness, surface and.or grain boundary scattering, all of which scale with the film thickness in this range.

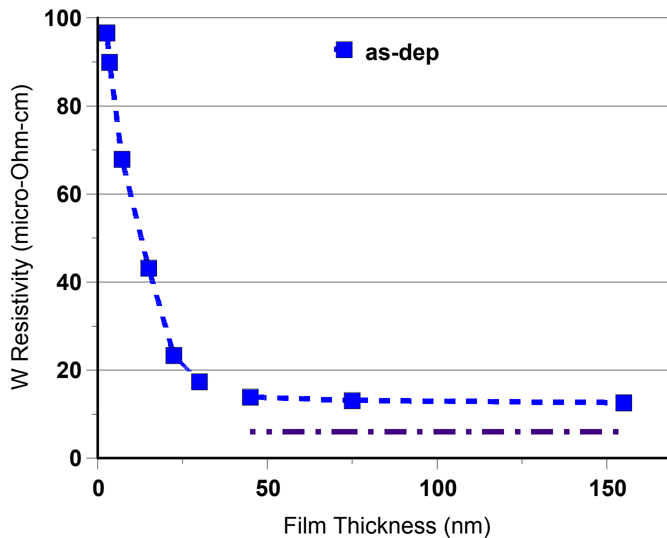

Figure 1. PVD W film resistivity as a function of film thickness, comparing as-deposited films (dashed line). The bulk value is shown at 5.3 micro-Ohm-cm.

The microstructure of the as-deposited films was completely alpha-W for films of 45 nm and greater thickness, beta-W for the thinnest sample (3.4 nm), and a mixture of alpha and beta phases for thicknesses between 3.4 and 45 nm.

These measurements of resistivity and structure were made immediately following the deposition. After a period of three days, the measurements were retaken to determine the effects of air

exposure and oxidation. However, instead of anticipated increases in film resistivity, the measured values dropped significantly for films in the mixed-phase range (3.4 < thickness < 45 nm). This is shown in Fig. 2. More detailed measurements of 7 and 15 nm films showed a monotonic decline in resistivity which may saturate after 10k minutes or so (Fig.3).

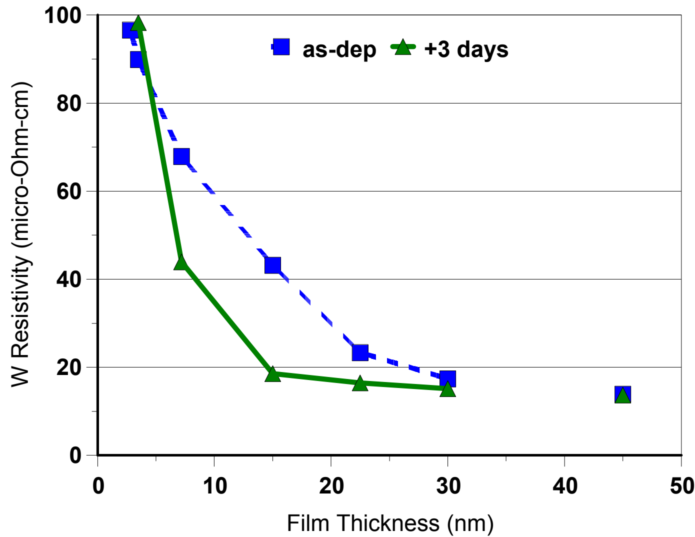

Figure 2. Resistivity of PVD W films as-deposited and 3-days post deposition (solid line) at room temperature. Films were deposited on wafer pieces lightly clamped to cooled backing plate.

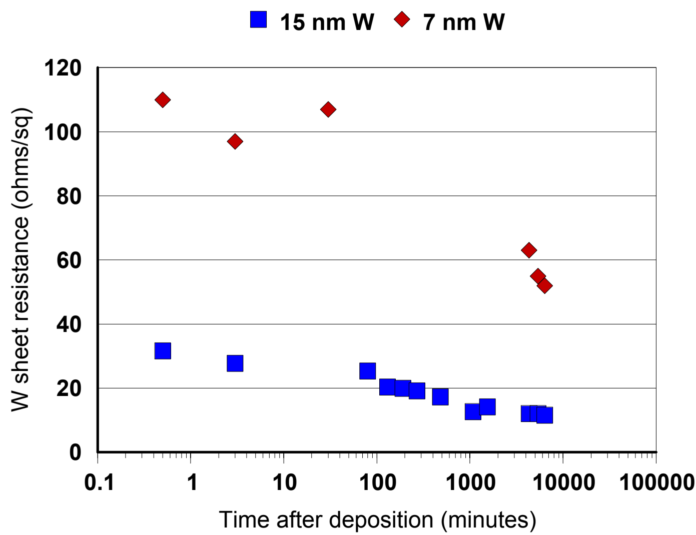

Figure 3. Sheet resistance (Ohms/square) of PVD W films following deposition at room temperature.

XRD measurements were taken concurrently with these same films, and showed an easily observable transition from a mixture of mostly beta and alpha W to entirely alpha W at the same terminal time as the completion of resistivity change (Fig. 4). While the 7 and 15 nm films showed no evidence of beta-W peaks after 10k minutes, the resistivity did not decrease

completely to the thick-film value (12 micro-Ohm-cm), due most probably to surface scattering effects or oxidation.

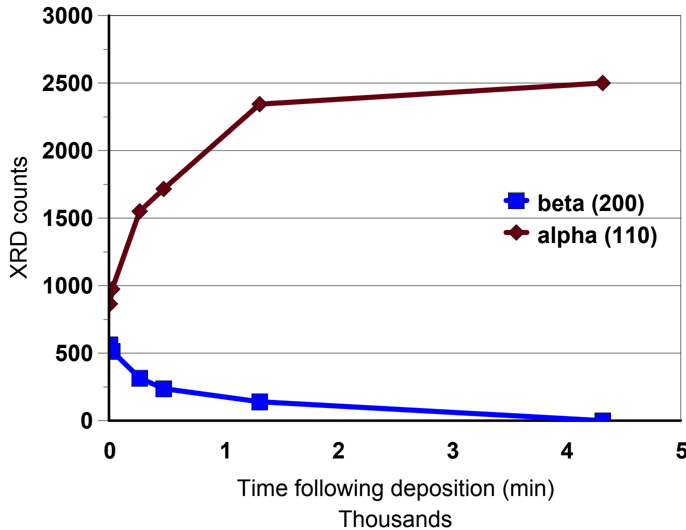

Figure 4. XRD peak heights (unnormalized) for 7 nm PVD W films following deposition.

W films of 7 and 15 nm thickness were then deposited at 250C by clamping samples to a heated wafer table. The resistivity of the as-deposited films was consistent with the terminal resistivity (5-10k minutes) for the unheated films. XRD measurements showed alpha-W only. There were no changes in these parameters over time.

W films were also deposited with intentionally-cooled substrates, clamped tightly to the holder at 18C. Films of 45 to 100 nm showed significant beta-W as-deposited and higher resistivity than observed with the earlier, less-well-cooled depositions. However, the films underwent similar beta-to-alpha transitions over the course of a several hundred to a few thousand minutes, and eventually attained the same alpha-only, bulk-like resistivities observed for the less-well-cooled films.

The effective activation energy for the phase transformation can be inferred by the use of the modified Kissenger analysis method (20,21). Thin (15 nm) as-deposited films were annealed in an He ambient at 4 different heating rates (from 1 to 27 deg C/sec). During the heating, the film's sheet resistance and XRD peaks were observed in-situ, and the transformation temperature from beta to alpha phase could be readily discerned by taking the derivative of the sheet resistance or XRD intensity as a function of temperature. The Kissenger analysis method relates the transition temperature to the heating rate (Fig. 5). A plot of $\ln\{(dT/dt)/T_m^2\}$ versus $1/kT_m$ has

a slope of -Q/n, where Q is the activation energy, n is the Avrami exponent, and k is Boltzman's constant (22).

The data for the sheet resistance change, the disappearance of the W-beta peak, and the abrupt increase in the W-alpha peak give an average activation energy of 1.1 +/- 0.2 eV. The error was estimated by the uncertainty of 3% in the heating ramp rate and a +/- 3 C error in temperature (22).

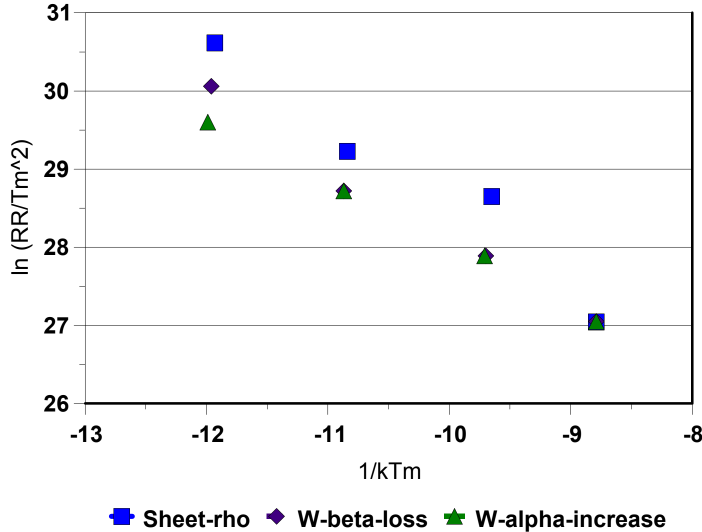

Figure 5. Modified Kissenger analysis method applied to beta-to-alpha phase transformation for 15 nm W films.

DISCUSSION

The transition of beta-W to alpha-W has been observed to be thermally driven (13), but generally at temperatures of >150C. Little work has been reported on room temperature transitions, particularly in the time range of 10 to 10,000 minutes. In addition, the correlation of oxygen contamination and the formation of the beta-phase has been observed repeatedly, as have the general effects of impurities on the resistivity of W (17-19). The current experiments address the issue of impurities in only an indirect manner. The 2x greater than bulk resistivity observed for the thick films (50-150 nm) may be due to systematic impurity contamination, since it does not appear to be thickness related. An impurity concentration of only a few percent of oxygen would be adequate to account for the increased resistivity. It was not possible to measure the impurity level of oxygen in these films without air exposure prior to measurement. High purity W for magnetron cathode fabrication is difficulty to obtain due to the very high melting point of the material. The current W target used was 99.95% pure, which is well below the purity levels of non-refractory materials, such as Cu or Al, which can be fabricated at 99.99999% purity levels.

As an indirect measure of the interaction between impurities and stabilization of the beta phase, depositions were undertaken with an increased chamber base pressure. When W films in the mixed-phase thickness range (3-45 nm) were deposited with a base pressure of 10^{-4} Torr (consisting mostly of water vapor), instead of 10^{-7} Torr, the beta-phase component of the films was very dominant, and neither the transition to the alpha phase at room temperature nor any changes in the electrical resistivity were observed following the deposition.

The correlation of reduced electrical resistivity with the transition from beta-W to alpha-W is consistent with reports of significantly higher resistivity for the metastable beta-phase (13).

Earlier studies of the deposition of W have suggested a minimum or critical thickness for the transition from beta to alpha W during the deposition process (12). Films thinner than the critical thickness are deposited as beta-W. After the critical thickness is reached, the existing beta is mostly converted to alpha, and subsequent deposition only occurs in the alpha phase. This model has been used to explain the 2 layer alpha-W thin film composites with different stress profiles (15). The current experiments suggest a slightly different effect which is only indirectly related to film thickness, and is driven by thermal effects.

The sputter deposition of high-atomic-weight materials, such as W and Ta, is complicated by the presence of (a) fairly energetic sputtered metal atoms, and (b) a significant flux of back scattered, neutralized Ar from the cathode surface. The energetic sputtered atoms have been measured by usually indirect means which date back to the 1960's (23,24). In general, the kinetic energy of the sputtered W and Ta atoms can exceed 10 eV/atom, and often exceeds 20 eV/atom. This may be due to the relatively low weight Ar ions and the 4-5x heavier target atoms.

The case of energetic, reflected neutrals has received considerable attention over the past 20 years. An extended series of papers by Hoffman and Thornton (25-27) examined the interplay between chamber pressure during sputter deposition and film properties, such as microstructure, stress, and adhesion. The case of low pressure (1-2 mTorr) sputtering of a high atomic weight target (W, Ta) by a low atomic weight gas species (Ar) leads to significant energy deposition at the film surface due to energy arriving via these reflected Ar neutral atoms, which can have several hundred eV of kinetic energy per particle.

The net result of these two effects is that the average effective energy deposited per arriving W atom can exceed many 10's of eV/atom. In the current experiment at a deposition rate of 73 nm/min, the heating rate during W deposition for a 0.6 mm thick silicon wafer sample, assuming 25 eV net energy/depositing atom and only minimal cooling through the back of the sample will be 0.4 to 0.7 C/sec. Therefore, after a deposition thickness of 45 nm under these conditions, the film surface temperature can exceed 125C just due to the kinetics of the deposition. Additional energy is also delivered during the deposition process to the film in the form of the heat of condensation of each W atom as well as various heat sources from the plasma used for the sputter deposition. As observed by earlier authors, this calculated temperature at 45 nm film thickness is the same temperature that would rapidly drive the beta-to-alpha transition for W films (13). Therefore, the earlier-observed critical thickness for the transition of beta to alpha W films is more likely a heating effect which is driven by the deposition process itself. The

observation of beta phase peaks in 100 nm films deposited with greater backside cooling is consistent with this conclusion. These observations also indicate that the thermal contact of the substrate with the substrate holder is of critical importance in the deposition of thin refractory films. Films deposited in the same machine, simultaneously or under identical deposition parameters can exist in different phases, or have different transformation rates, only by virtue of having better thermal transfer between the film and the substrate.

The data of Fig. 2 for the post-transformed alpha W are indicative of a fairly small electron mean free path for W. Earlier reports in the literature (1, and references therein) give a mean free path of 41 nm. However, from the scaling of Eqns (1) and (2), the electrical resistivity of the film should increase by a minimum of 38% at a thickness equal to the mean free path, and most likely much more due to the additive surface roughness and grain boundary effects. The scaling of Fig. 2 for the alpha-phase material (solid line in Fig. 2) shows a nearly flat resistance from 150 nm to less than 20 nm, which suggests an electron mean free path of 10-12 nm.

CONCLUSIONS

Thin W films, deposited by magnetron sputtering, were deposited on silicon-dioxide surfaces at near-room temperature at thicknesses from 3 to 150 nm. Films below 45 nm thickness showed evidence of metastable beta-phase W which changed to alpha-phase in a period of hours to days at room temperature, and faster at elevated temperature. Films > 45 nm thickness, when deposited with better cooling, showed evidence of beta-phase W which then changed to alpha phase in 10s of hours with an average activation energy of 1.1 +/- 0.2 eV. This suggests, along with calculations of the energy flow to the sample, that there is no critical thickness for alpha-phase deposition. Thicker films are simply at higher temperature due to the deposition, and the increased temperature drives the beta-to-alpha transition. Finally, due to the scaling of the alpha-phase resistivity with thickness, the mean-free-path for electrons in W appears to be in the range of 10-12 nm, far below the published value of 41 nm. This will have some impact on the functional resistance of W films used for very thin, liner applications.

Acknowledgements: The work completed at the National Synchrotron Light Source at Brookhaven National Laboratory was conducted under DOE contract DE-AC02-76CH-00016.

REFERENCES

1. A. J. Lean and D. W. Foster, J. Appl. Phys., **58** (1985) 2001.
2. D. Edelstein et al, IITC Proceedings, Burlingame, CA 6-4-01.
3. S. M. Rossnagel, D. Mikalsen, H. Kinoshita and J. Cuomo, J. Vac. Sci. & Technol., **A9** (1991), 261.
4. A. Mayo, S. Hamaguchi, J. H. Yoo, and S. M. Rossnagel, J. Vac. Sci. & Technol., **B15** (1997), 1788.
5. S. M. Rossnagel, C. Nichols, S. Hamaguchi, D. Ruzic and R. Turkot, J. Vac. Sci. & Technol., **B14** (1996) 1819.
6. S. M. Rossnagel and J. Hopwood, Appl. Phys. Lett. **63** (1993), 3285, S. M. Rossnagel and J. Hopwood, J. Vac. Sci. & Technol., **B12** (1994), 449.

7. S. M. Rossnagel, Thin Solid Films, **263** (1995) 1.
8. S. M. Rossnagel, J. Vac. Sci. & Technol. **B16** (1998) 2585.
9. P. F. Cheng, S. M. Rossnagel and D. Ruzic, J. Vac. Sci. & Technol., **B13** (1995) 203.
10. C. Kittel, Introduction to Solid State Physics, (John Wiley and Sons, 1953, New York), Chapter 7.
11. T.S. Kuan, C. K. Inoki, G. S. Oehrlein, K. Rose, Y.-P. Zhao, G. -C. Wang, S. M. Rossnagel and C. Cabral, Mat. Res. Sco. Symp. Proc. Vol **612** (2000) D7.1.1.
12. I. C. Noyan, T. M. Shaw, and C. C. Goldsmith, J. Appl. Phys., **82** (1997) 4300.
13. P. Petroff, T .T. Sheng, A. K. Sinha, G. A. Rozgonyi and F. B. Alexander, J. Appl. Phys. **44** (1973) 2545.
14. I. A. Weerasekara, S. I. Shah, D. V. Baxter, and K. M. Unruh., Appl. Phys. Lett. **64** (1994) 3231.
15. T. J. Vink, W. Walrave, J. C .L. Daams, A. G. Dirks, M. A. J. Somers, and K. J. A. Van der Aker, J. Appl. Phys. **74** (1993) 988.
16. L. Krusin-Elbaum, K. Ahn, J. H. Souk, C. Y. Ting and L. A. Nesbit, J. Vac. Sci. & Technol. **A4** (1986) 3106.
17. J . Ligot, S. Benayoun and J. J. Hantzpergue, J. Vac. Sci. & Technol. **A19** (2001) 798.
18. C. E. Wickersham, J. E. Poole and K. E. Palme, J. Vac. Sci. & Technol., **B4** (1986) 1339.
19. F. Meyer, D. Bouchier, V. Stambouli, C. Pellet, C. Schwebel and G. Gautherin, Appl. Surf. Sci., **38** (1989) 286.
20. S.-L Zhang and F.M. D'Heurle, Thin Solid Films, **256** (1995) 155.
21. P. G. Boswell, J. Thermal Anal. **18** (1980) 256.
22. C. Cabral. Jr., P. C. Andricacos, L. Gignac, I.C. Noyan, K.P. Rodbell, T.M. Shaw, R. Rosenberg, J.M.E. Harper, P.W. DeHaven, P.S. Locke, S. Malhotra, C. Uzoh and S.J. Klepsis, Proc. ULSI XIV (1999, Materials Research Society) 81.
23. J. A. Thornton and J. L. Lamb, Thin Solid Films **119** (1984) 87.
24. G. K. Wehner, Phys Rev. **114** (1959) 1270.
25. D.W. Hoffman and J.Thornton, Thin Solid Films, **40** (1977) 355.
26. J.A. Thornton and D. W. Hoffman, J. Vac. Sci. & Technol., **18** (1981) 203.
27. J. A. Thornton and D. W. Hoffman, J. Vac. Sci. & Technol., **A3** (1985) 576.